(CONFIDENTIAL)

Office of Scientific Research and Development
Section 6.1 - National Defense Research Committee

THE HIGH SPEED WATER TUNNEL
at the
CALIFORNIA INSTITUTE OF TECHNOLOGY

MEMORANDUM ON WATER TUNNEL TESTS OF A 2.37" ROCKET PROJECTILE WITH COLLAPSIBLE TYPE TAILS

(Laboratory Designation, HD-11)

by

Robert T. Knapp
Official Investigator

California Institute of Technology
Hydraulic Machinery Laboratory
Pasadena, California

Section No.
NDRC Rep. No. HD-11.1
Copy No. 16

January 20, 1943

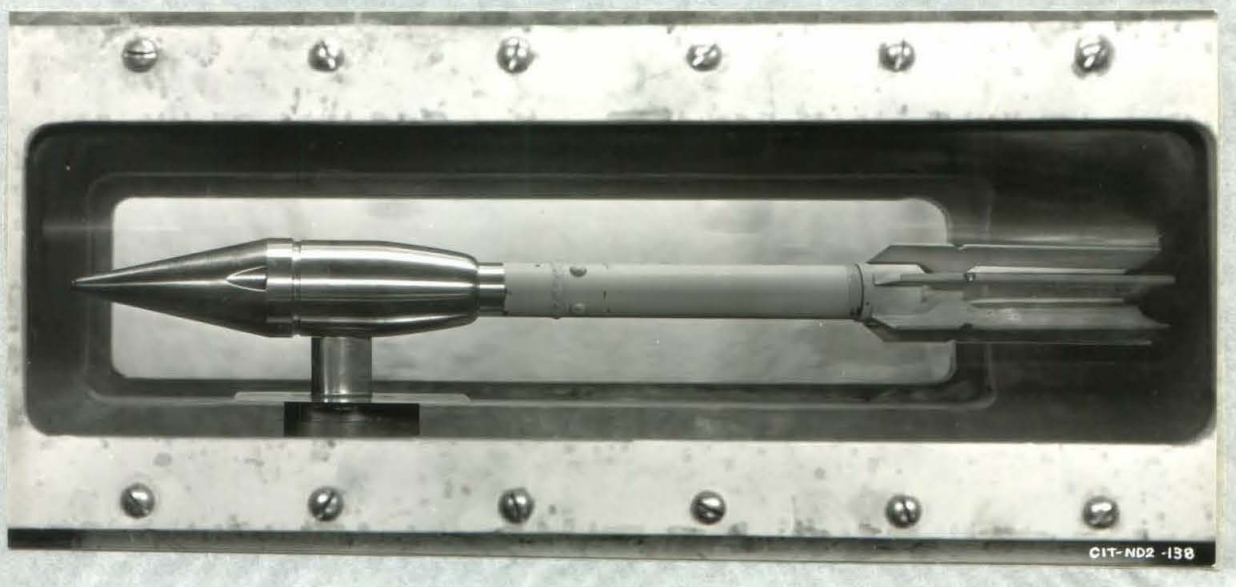

Figure A - 2.37" Rocket Projectile
Shown Mounted in Water Tunnel Working Section

Figure 1. - Rocket Projectile with Original Fixed Fin Tail.

Figure 2. - Rocket Projectile with Collapsible Tail #2 (Medium 90°) Tail fins are shown in folded position for firing.

Figure 3. - Rocket Projectile with Collapsible Tail #2 (Medium 90°)
Tail fins are shown in the unfolded position assumed during flight. Note the inclination of the fin tabs with respect to the direction of motion.

Figure 4. - Rocket Projectile with Collapsible Tail #3 (Medium Raked)
Tail fins are shown in the unfolded position assumed during flight. Note how the fin tabs line up with the direction of motion. (Compare with Figure 5)

Figure 5. - Construction Details of Collapsible Tail #1 (Short 90°) Note the fin attaching ring construction. (Compare with Figures7 and 8)

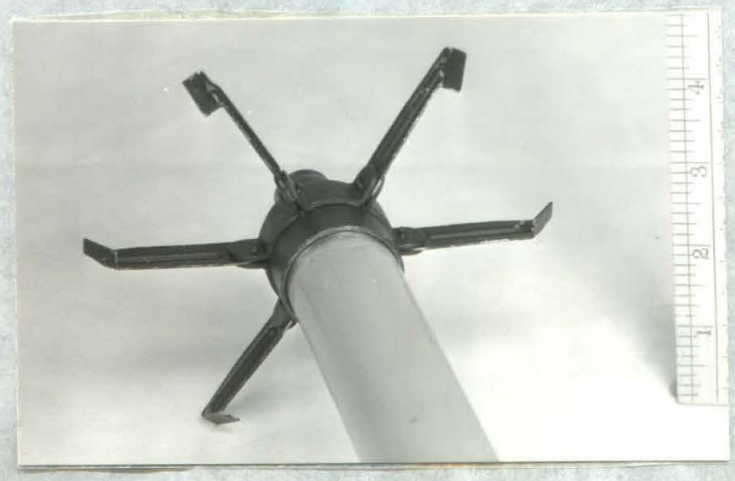

Figure 6. - Construction Details of Collapsible Tail #1 (Short 90°). Note the fin attaching ring construction. (Compare with Figures 7 and 8)

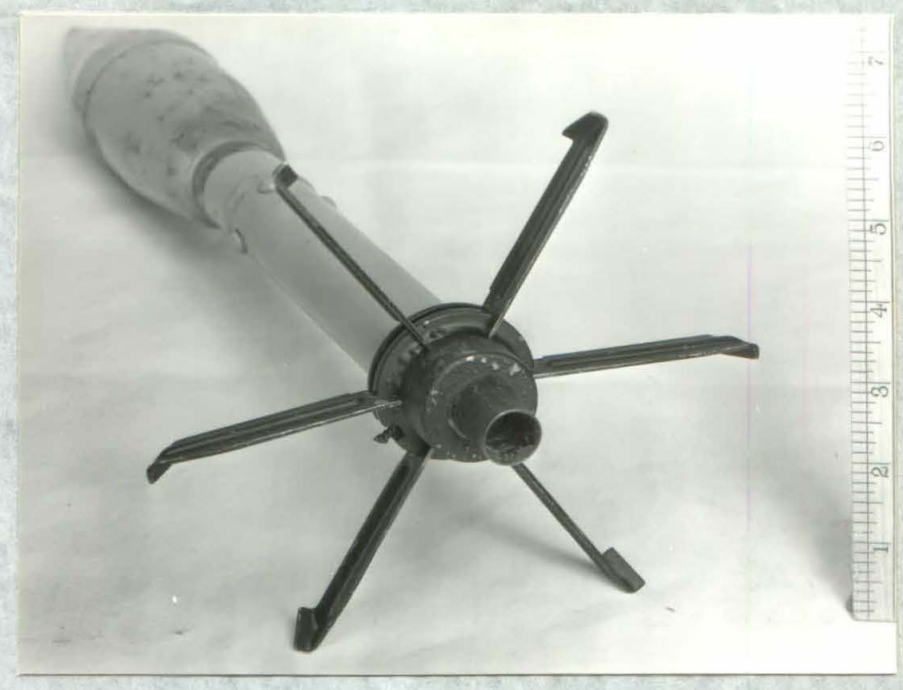

Figure 7. - Construction Details of Collapsible Tail #2 (Medium 90°) Note the fin attaching ring construction. (Compare with Figures 5 and 6)

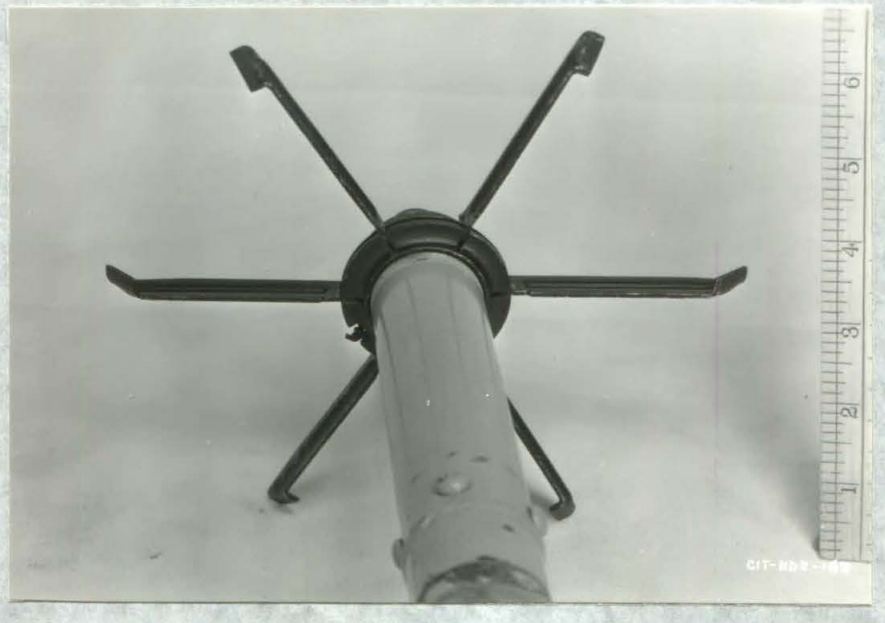

Figure 8. - Construction Details of Collapsible Tail #2 (Medium 90°) Note the fin attaching ring construction. (Compare with Figures 5 and 6)

Figure 11. - Construction Details of Collapsible Tail #4 (Long Naked). Note the thin blade fins. (Compare with Figures 5 to 10)

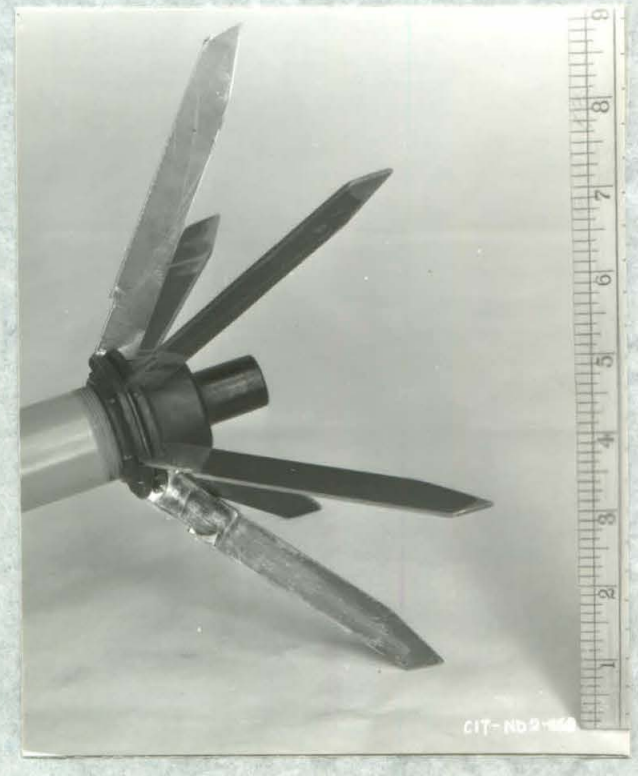

Figure 12. - Construction Details of Collapsible Tail #4 (Long Naked)

Figure 9. - Construction Details of Collapsible Tail #3 (Medium Raked). Note pressed rib and end tab for each fin. (See also Figures 5 to 8)

Figure 10. - Construction Details of Collapsible Tail #3 (Medium Raked).

MEMORANDUM ON WATER TUNNEL TESTS OF A 2.37" ROCKET PROJECTILE WITH COLLAPSIBLE TYPE TAILS (Laboratory Designation ND-11)

1. Type of Projectile and Purpose of Tests

This report covers water tunnel tests of a full scale 2.37" rocket projectile (designated in the laboratory as projectile number ND-11 Impervium) with four different collapsible tails. The purpose of the tests was to compare the drag coefficients for this projectile using each of the collapsible tails with the drag coefficient for the projectile using its original fixed-fin tail,(1) and to determine the effect of the collapsible type tail on the center-of-pressure location.

2. Tunnel Installation and Description of Forces Measured

The tests were conducted in the 14" diameter working section of the High Speed Water Tunnel at the California Institute of Technology.(2) Figure A shows the projectile installed in the tunnel. In order to reduce the drag tare to a minimum, the rigid supporting spindle is protected from the flow by the streamline shielding shown in the figure. This shielding which projects to within a few thousandths of an inch of the projectile is held to a small size in order to reduce interference effects.

The forces exerted by the flow on the model can be resolved, in general, into a drag force parallel to the flow, a cross wind force normal to the flow, and moment or torque acting about the point of support. These are the forces measured during test. The moment exists only if the model is not supported at the point of application of the resultant of all the hydrodynamic forces. It is clear that the magnitude and sense of the measured moment will change if the point of support is shifted along the body.

The Water Tunnel tests give results which are applicable in either air or water for velocities below that of sound. For velocities in the neighborhood or above that of sound the results will not apply.

3. Representation of Test Data

The hydrodynamic characteristics are presented in the form of curves of force coefficients as functions of the angle of yaw. In addition, the distance of the center-of-pressure from the nose of the projectile expressed as a fraction of the length of the projectile is plotted against yaw angle. The center-of-pressure is defined as the point at which the resultant hydrodynamic force vector intersects the axis of symmetry of the model.

The force coefficients, C_D, for drag and, C_C, for cross wind force are expressed as:

$$C_D = \frac{D}{\rho \frac{V^2}{2} A_D}$$

and

$$C_C = \frac{C}{\rho \frac{V^2}{2} A_D}$$

where

D = measured drag force in lbs

C = measured cross wind force in lbs

ρ = density of water in slugs per cu ft

A_D = area in sq ft of a cross section at the cylindrical portion of the projectile head taken normal to the geometric axis of the projectile (= 3.98 sq in, i.e. dia = 2.25 in, for this projectile)

V = mean relative velocity between thewater and the projectile in ft per sec

The moment coefficient is expressed as:

$$C_M = \frac{M}{\rho \frac{V^2}{2} A_D L}$$

where

M = moment in in-lbs measured about any particular point on the geometric axis of the projectile

L = overall length of the projectile in in. (For all combinations of the projectile discussed in this report L is taken as 21 3/8")

The distance from the nose to the center-of-pressure (center-of-pressure distance) as a fraction of theoverall projectile length is expressed as:

$$\frac{X}{L} = \frac{L' + L''}{L} = \frac{L'}{L} + \frac{1}{L}\left(\frac{M}{C \cos \psi + D \sin \psi}\right)$$

where

L' = distance in in from the projectile nose to the center of moments

L" = distance in in from the center-of-pressure to the center of moments

ψ = yaw angle in degrees

When M is the measured moment the center of moments is at the support point of the model and L" then is the distance from the support point to the center-of-pressure. The signs of the moment, M, the cross wind force, C, and the yaw angle, ψ , are such that M and ψ have the same sign when they oppose each other and C and ψ have the same sign when they act in the same direction. Thus, for example, a positive or clockwise moment will tend to reduce a positive or counter clockwise yaw angle, while the corresponding positive cross wind force will act to the left. (when facing in the direction of the trajectory)

4. Discussion of Interpretation of Test Results from Assymetrical Projectiles

Figure 13 shows typical coefficient curves for this rocket projectile tested with its original fixed-fin tail. The coefficients and center-of-pressure distances are plotted as functions of the yaw angle measured with respect to the geometric axis of the projectile. It will be noted that the curves are not symmetrical for positive and negative yaw angles and furthermore, that the cross wind and moment coefficients have finite values at zero angle. It is believed that these effects are primarily the results of non-symmetrical model construction. Such effects are the cause of the different center-of-pressure distance curves for positive and negative angles.

Care must be taken in the interpretation of these results. The curves show that for a yaw of about -0.35 degrees, the value of the cross wind force, C , is zero, and that the moment, M, has an appreciable negative value. Since for small angles the distance, L" , from the support to the center-of-pressure is given very closely by M/C, it is easy

to see that a discontinuity occurs where C goes to zero. It is also easy to see that as we cross the point of discontinuity, moving from left to right, the sign of M does not change, while that of C does change, thus causing the center-of-pressure to move from a point at some distance behind the center-of-gravity of the projectile to considerably forward of the centroid.

The fact that M/L becomes very large so that the center-of-pressure falls outside the projectile does not necessarily mean that the projectile is unstable. This can be explained by examining the moment coefficient curve while keeping in mind the meaning of the moment sense convention. For large negative angles the negative couple tends to reduce the yaw. The negative sense of this couple persists past zero yaw and up to a positive yaw angle of +2.4°. At this point the moment vanishes. Thus for the entire negative range of and for this small positive zone the moment tends to rotate the projectile toward the yaw angle of +2.4°. For yaw angles greater than +2.4 degrees the couple has a positive sense and tends to oppose further increase in the yaw. Thus the yaw angle of +2.4 degrees is the neutral or equilibrium position at which the projectile should be stable. From the fact that a finite side force exists when the couple is zero, it is expected that the projectile will "side slip."

The same interpretation is obtained from the M/L curves if the sense of the cross wind force is kept in mind. However, for these particular test results, it is more convenient to use the moment curves. In the case of symmetrical shapes there is a fixed relation between the senses of the yaw angle and the cross wind force, and the senses of the yaw angle and the moment. As a result the center-of-pressure distance curves give a straight forward picture of the action of these forces.

Figure 13 showed the characteristics of a particular model which had been yawed in only one plane. Experiments have shown that for asymmetric models the characteristics vary appreciably for different yaw planes. The paths of such projectiles will therefore vary depending on how the yaw shifts from one plane to another and a very complicated motion can be expected.

The behavior of the asymmetric projectile discussed above is probably typical of many projectiles, since experience has indicated that the construction of a projectile with perfect symmetry is very difficult even for laboratory models made in precision work shops. However, it cannot be said with assurity that such information is quantitatively representative of a large group of projectiles without careful consideration of the behavior in several planes of yaw and without knowing the probable limits of misalignment and asymmetry to be encountered. In addition, it is difficult to use results which are influenced by so many variables. Thus the characteristics of a perfectly symmetrical projectile are to be preferred since they are

easy to use and since they are likely to indicate the average performance of a number of projectiles with as much accuracy as does the data for non-symmetrical behavior.

Since none of the rockets tested for this report was symmetrical, an approximation of the characteristics for symmetry was prepared using the test data as a basis for the estimates. In the case of drag the effect of asymmetry is slight so that an average of the values for positive and negative yaw angles is satisfactory. An examination of all the data showed that a similar treatment was probably good for the cross wind force if the yaw angle origin was first translated to that where C = 0. The treatment of the moment and $\overline{x}/L$ curves is not so clear cut. However, many tests made by rotating the projectile tail with respect to its head, showed that the slopes of the nearly linear cross wind and moment curves assumed reasonably constant values, especially near the origin. The effect of the change in asymmetry introduced by the tail rotation merely shifted the C and M intercept on the yaw angle axis. Using these slopes the center-of-pressure distance at $\psi = 0$ was determined. As indicated on Figure 13 this value agreed closely with the average value of the two brances of the actual $\overline{x}/L$ curve, and with the value which both branches apparently assume at large yaw angles where the asymmetry effects are relatively reduced. Fairing gives a constant value to the $\overline{x}/L$ curve approximated from these conditions. Using this approximated $\overline{x}/L$ and the faired values for C_D and C_C a curve of C_M can be calculated for this assumed symmetrical condition. Figure 14 shows, the symmetrical coefficient and center-of-pressure distance curves for the fixed-fin projectile obtained by following the procedure just outlined. The significant difference between the behavior described by Figure 13 and that given by Figure 14 is that the neutral or zero moment condition has been shifted from +2.4° to zero yaw.

5. Description of Tails

Figure 1 is a photograph of the projectile with its original fixed-fin tail and Figures 2 and 3 show the projectile with collapsible tail No. 2. Since the bore diameter of the firing equipment for this projectile is fixed the collapsible tails were designed to have the same maximum radial dimension in the folded position as the original tail. This is shown clearly by comparing Figures 1 and 2. In flight the fins unfold to a fixed radial position of either 90° (approximately) with respect to the projectile axis or raked back from the 90° position. Figure 3 shows tail No. 2 in the unfolded position. Figure 4 shows tail No. 3 which is of the same construction, except that the fins are raked back from the 90° position. The four tails tested included two with 90° fins, (No. 1 and No. 2), and two (No. 3 and No. 4) with raked fins. There were three sizes as measured by the length of the fins. The main dimensions are given in Table I:

Table I

Description of Tail	Vanes Folded Max. Span Inches	Vanes Unfolded Max. Span Inches	Angular Position of Fins Degrees Back From Radial	No. Of Fins	Type Of Fins	Length Of Fins Inches
Short 90°, #1	2 9/32	5 3/8	8°	6	Pressed Steel	1 7/8
Medium 90°, #2	2 5/16	7 1/4	5°	6	"	2 3/4
Medium Raked, #3	2 5/16	5 7/8	40°	6	"	2 3/4
Long Raked, #4	2 3/8	8	40°	6	Straight Thin Blades	4 7/16

Figures 5 to 12 inclusive show the construction details of the four tails. Note that two different types of fins are used. One type, shown only on the tail No. 4 in Figures 11 and 12, is a long thin blade of steel. The second type used on the other three tails is made of pressed steel with a hollow rib along its length and a short tab at the end. As shown in Figures 5 and 6 this tab is bent into a plane normal to the plane of the fin and at 45° to the longitudinal axis of the fin. The plane of the tab consequently is inclined to thedirection of motion for the 90° tails and is lined up with the direction of motion for the Raked Tails. The fins are mounted on the boom or motor housing of the projectile by means of retaining wires and attaching rings. The attaching rings are of two types one of which is illustrated by Figures 5 and 6 and the other by Figures 7 and 8.

6. Test Results

Figure 15 shows coefficient and center-of-pressure location curves for the four collapsible tails and for the fixed-fin tail. The curves were approximated by averaging and fairing the t est data as explained in Section 4 of this report. For two of the collapsible tails only the drag at zero yaw is given, while for the other two units the coefficients and the center-of-pressure distances are given. The curves are plotted as functions of the angle of yaw with respect to the geometric axis of the projectile. All values of the center-of-pressure distance $\bar{x}/L$ are referred to an overall length of 21 3/8", the length of the projectile using the original fixed-fin tail. The moment coefficients are calculated with respect to the center of gravity of the projectile. The distances from the nose to the center-of-gravity for the projectile with each of three tails are given in Table II. These are approximate values calculated for the case where the motor powder is fully expended.

Table II

Description Of Tail	Distance from Nose to Center of Gravity	
	Inches	As Fraction of 21 3/8"
Fixed-Fin	9.62	0.45
Short 90°, #1	9.19	0.43
Medium 90°, #2	9.41	0.44

The collapsible tails cause the center-of-pressure distance from the projectile nose to be increased a small amount. The change is slight, however, and assumes significance only when considered in terms of the simultaneous shift of the center of gravity. As Table II shows, both the Short 90° and Medium 90° tails cause the center-of-gravity to move forward. If the margin for stability is measured in terms of the distance between the center of gravity and center-of-pressure, the C.G. shift forward combined with the C.P. movement rearward represents an increase in stability over the fixed-fin tail. Within the probable limits of accuracy of the test data and fairing methods the difference between $\bar{X}/L$ values for the Short 90° and Medium 90° tails is not significant. Actually, the smaller weight of the Short 90° causes the center-of-gravity to be further forward than for thelatter. Therefore, the Short 90° type possesses a slightly greater margin for stability. Figure 16 shows graphically the positions of the center-of-gravity and the center-of-pressure for each of the three tails. Since for the fixed-fin tail the distance between the C.P. and C.G. is very small even a slight increase in this distance may have an appreciable effect on the stability.

A comparison of the drag coefficients given on Figure 15 shows a 40% to 300% increase in C_D when the collapsible tails are used in place of the fixed-fin tail. These high drag coefficients will reduce the maximum velocity and the range of the projectile. The highest value of 0.95 is for tail No. 2, the Medium 90° type. The Short 90° tail, tail No. 1, gives a value of only 0.52. This very large difference is caused by the construction features of the fin attaching ring used with tail No. 2. As seen by comparing Figures 5 and 7 the projected area of the ring to which the fins of No. 2 tail are attached offers extra obstruction and interference to the relative flow past the projectile. This is verified by Table III which gives the total projected area of each tail normal to the direction of motion.

Table III

Description of Tail	Projected Area of Tail Normal to Direction of Motion	Estimated Total Drag Coefficient	Measured Drag Coefficient
	sq in		
Fixed-Fin	0.45		.30
Short 90°, #1	2.00	.57	.52
Medium 90°, #2	3.76	.98	.95
Medium Raked, #3	2.92	.73	.76
Long Raked, #4	2.69	.69	.77

Table III also shows values of estimated and measured drag coefficients. The estimates were obtained by first subtracting from the measured total drag of the projectile with the fixed-fin tail the estimated drag of the tail to give the drag of thehead and boom alone. Then, by adding to this drag for thehead and boom the estimated drag of the various collapsible fin tails, the estimated total drag coefficients shown in Table III were obtained. The estimates of tail drag are based on a coefficient of 0.7 applied to the projected areas of thetails. The remarkable agreement between the measured and estimated drag coefficients, indicates that this simple method offers good possibilities for evaluating, roughly, the effects of further modifications.

In summary it is clear that the collapsible tails produced small but beneficial changes in the location of the C.P. and C.G. but at the same time the drag force was increased materially. It is also probably true that the collapsible tails are more complicated to build and to use than the fixed-fin tails. The extremely high drag is not necessarily inherent in the design of the collapsible tail and can be reduced. The procedure to follow in reducing the drag is suggested in the analysis of Table III and is to first minimize the projected area and then to reduce the drag coefficient of the final profile by fairing. Considerable progress in this direction has been made in the case of the small 90° tail. Further improvements could be made by lining up thetail tabs with the flow and by fairing the front and after part of the nozzle fitting. The mechanical complication is inherent in the collapsible type tail and can be eliminated only by adopting a simple fixed tail.

If more stabilizing is required than the fixed-fin tail gives

then it will be necessary to make some fundamental change in the tail design. It should be possible to achieve this with a ring tail.* Other projectiles with streamlined heads, similar booms and ring tails with relatively large fin surfaces, have given comparatively large values of $\frac{W}{L}$ with drag coefficients as low as 0.15.

It should be remembered that the test results and discussion presented for these collapsible tails apply to symmetrical projectiles. As was emphasized in Section 4 of this report, asymmetry in the construction of the rocket can be expected to cause a very complicated motion in flight and certainly must introduce extra dispersion or scatter when the rocket is fired. For this reason it is recommended that considerable thought be given to methods of obtaining symmetry.

References:

(1) For a complete description of tests of this projectile with its original fixed-fin tail see the report "Memorandum on Water Tunnel Tests of a 21 3/8" Rocket Projectile," by H. T. Knapp, HML-Rep. No. ND-11, November 19, 1942.

(2) For complete description see the following report on file in the office of Section 6.1, NDRC, "The High Speed Water Tunnel at the California Institute of Technology," by R. T. Knapp, V. A. Vanoni and J. W. Daily, June 29, 1942.

* A ring tail is made with a cylinder of thin metal and radial fins which fasten to the after body or boom and hold the cylinder so its axis coincides with that of the projectile.

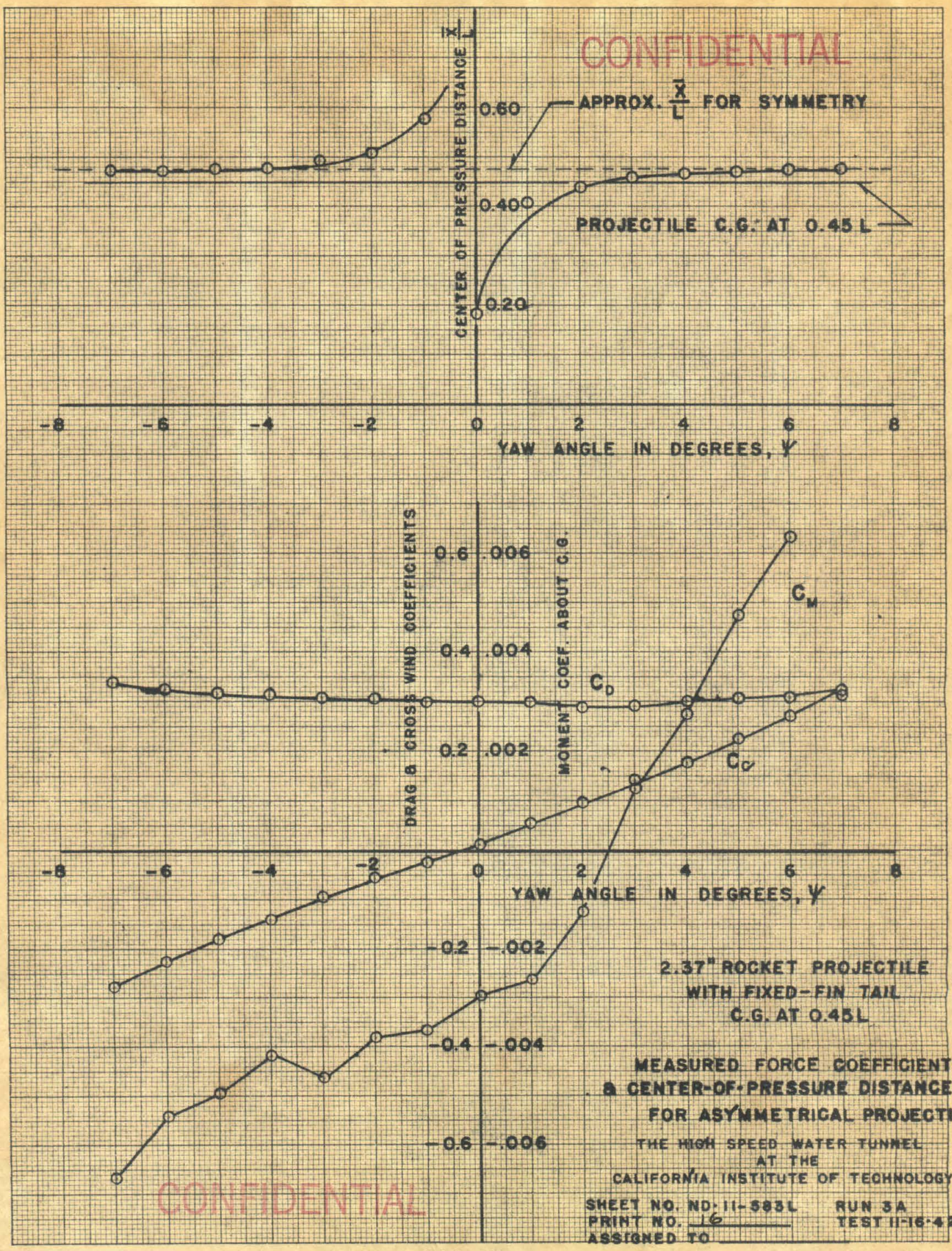
CONFIDENTIAL
CENTER OF PRESSURE DISTANCE $\frac{\bar{X}}{L}$
0.60
APPROX. $\frac{\bar{X}}{L}$ FOR SYMMETRY
0.40
PROJECTILE C.G. AT 0.45 L
0.20
-8 -6 -4 -2 0 2 4 6 8
YAW ANGLE IN DEGREES, ψ
DRAG & CROSS WIND COEFFICIENTS
MOMENT COEF. ABOUT C.G.
0.6 .006
0.4 .004
0.2 .002
C_M
C_D
C_C
-8 -6 -4 -2 0 2 4 6 8
YAW ANGLE IN DEGREES, ψ
-0.2 -.002
-0.4 -.004
-0.6 -.006
2.37" ROCKET PROJECTILE
WITH FIXED-FIN TAIL
C.G. AT 0.45L
MEASURED FORCE COEFFICIENTS
& CENTER-OF-PRESSURE DISTANCES
FOR ASYMMETRICAL PROJECTILE
THE HIGH SPEED WATER TUNNEL
AT THE
CALIFORNIA INSTITUTE OF TECHNOLOGY
SHEET NO. ND-11-583L RUN 3A
PRINT NO. 16 TEST 11-16-42
ASSIGNED TO
CONFIDENTIAL

FIG. 13

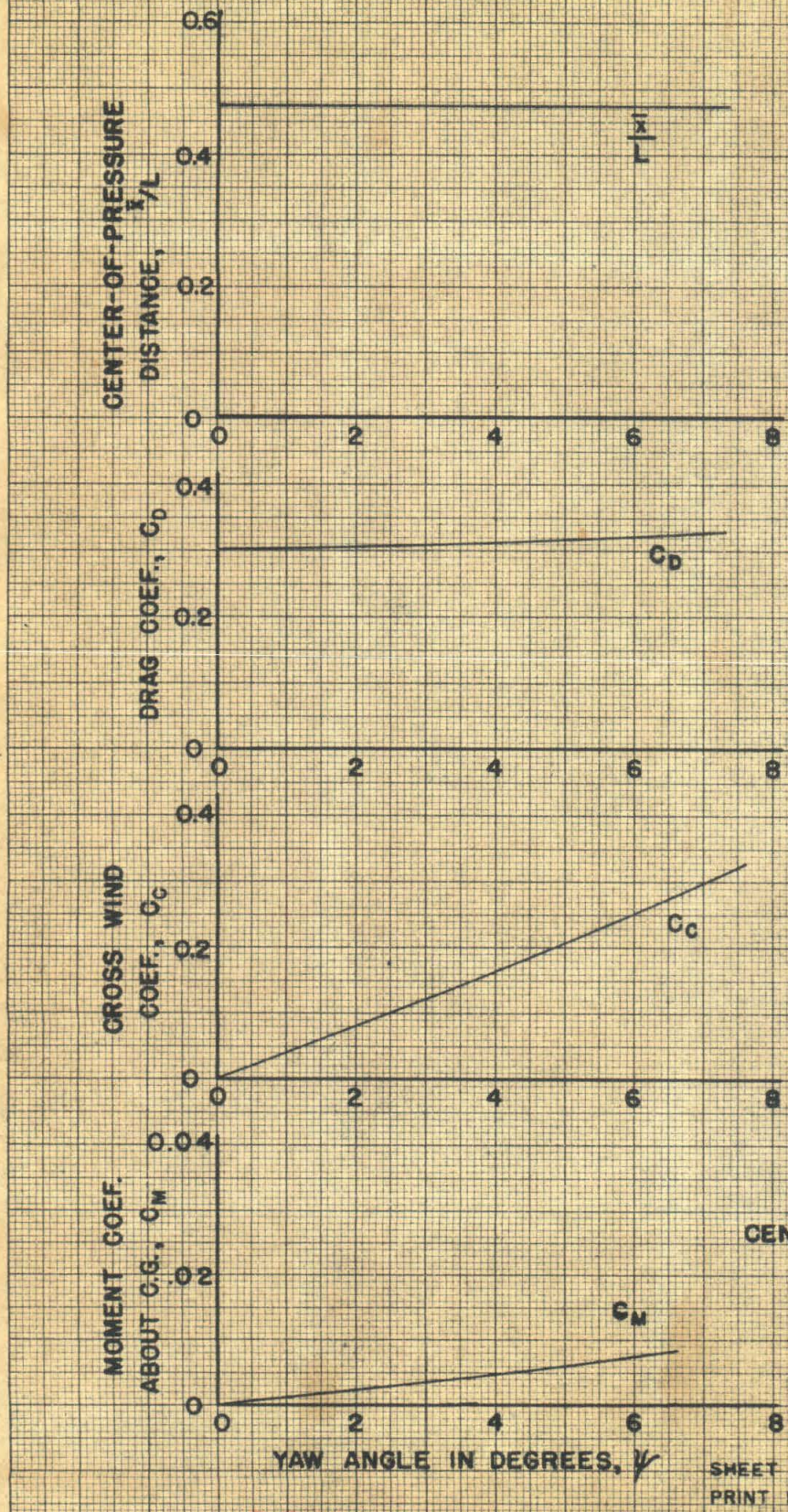

2.37" ROCKET PROJECTILE
WITH FIXED-FIN TAIL
C.G. AT 0.45L

FORCE COEFFICIENTS AND
CENTER-OF-PRESSURE DISTANCE
CALCULATED FOR
SYMMETRICAL PROJECTILE

THE HIGH SPEED WATER TUNNEL
AT THE
CALIFORNIA INSTITUTE OF TECHNOLOGY

SHEET NO. ND 11-582-L
PRINT NO. 16
ASSIGNED TO

RUN 3a
TEST 11-16-42

FIG. 14

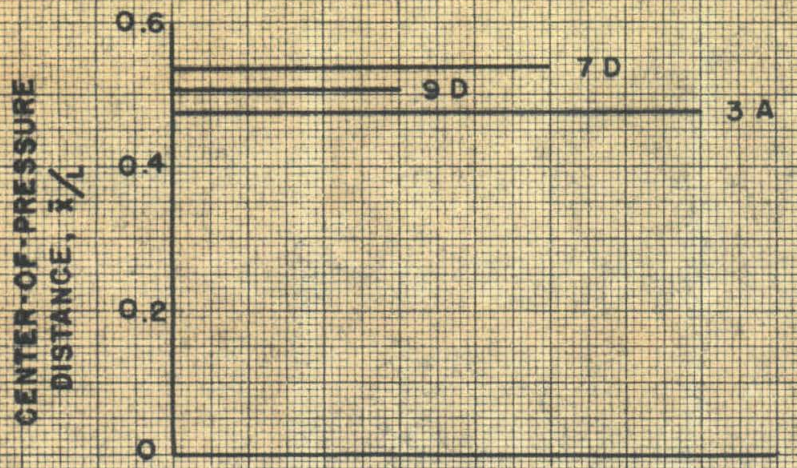

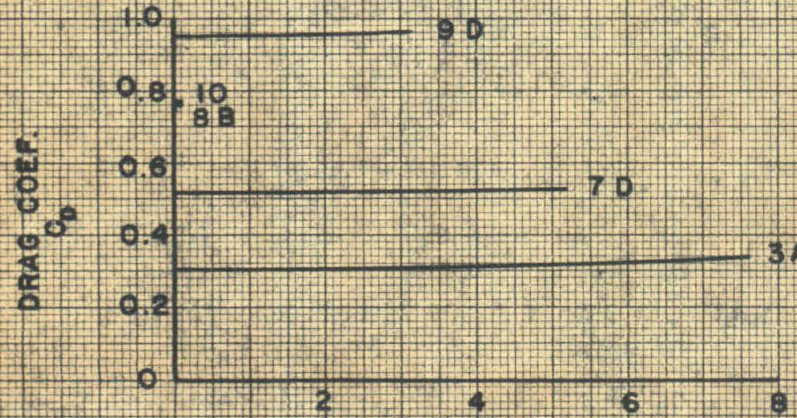

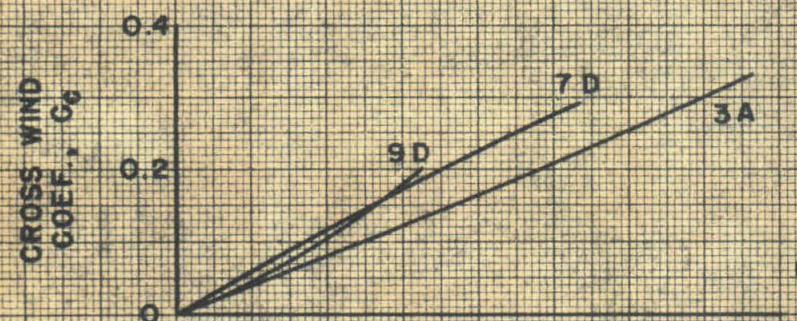

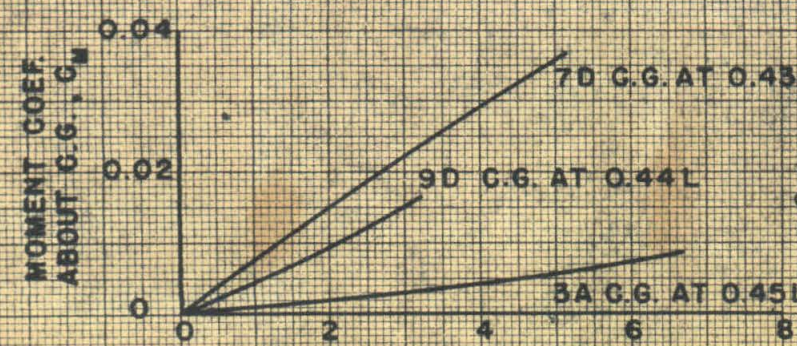

RUN 3A FIXED-FIN

RUN 7D SHORT 90°

RUN 8B MEDIUM RAKED

RUN 9D MEDIUM 90°

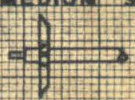

RUN 10 LONG RAKED

2.37" ROCKET PROJECTILE WITH FIXED-FIN AND COLLAPSIBLE TAILS

FORCE COEFFICIENTS AND CENTER-OF-PRESSURE DISTANCE CALCULATED FOR SYMMETRICAL PROJECTILE

THE HIGH SPEED WATER TUNNEL AT THE CALIFORNIA INSTITUTE OF TECHNOLOGY

SHEET NO. NOii-584-L RUNS 3A, 7D, 8B, 9D, 10
PRINT NO. 14 TESTS NOV.-DEC. 1942
ASSIGNED TO

FIG. 15

CONFIDENTIAL

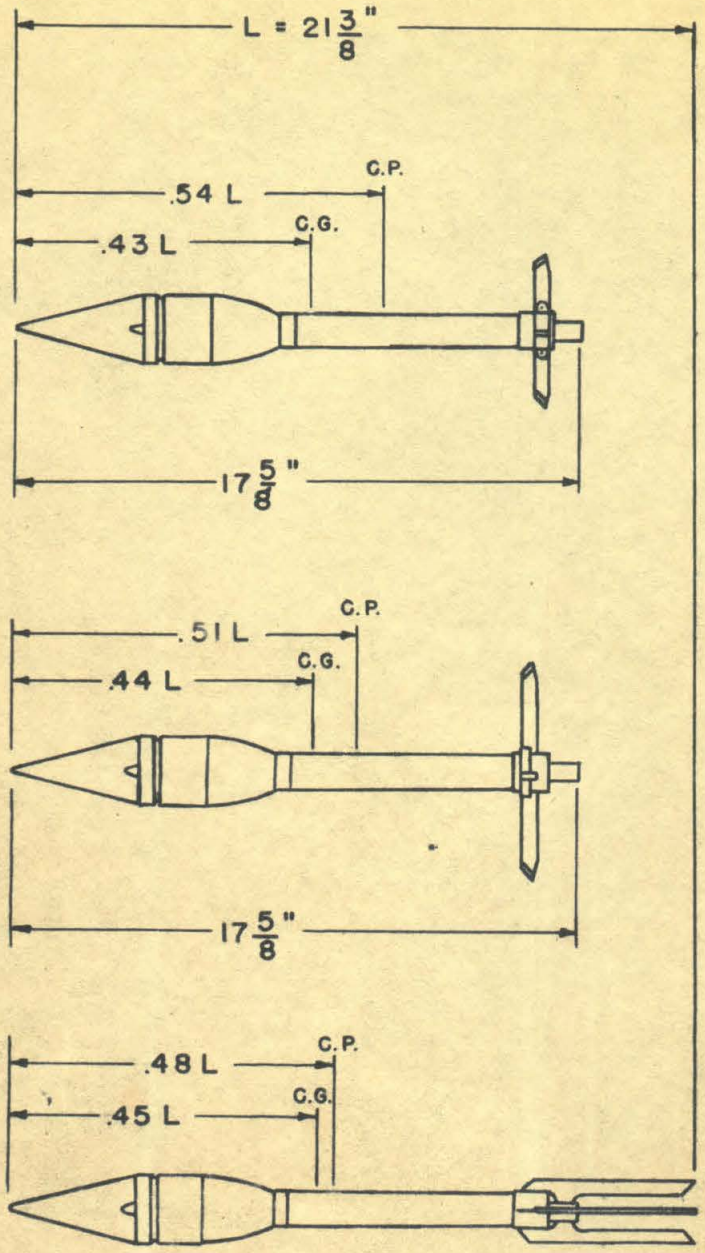

SMALL 90° TAIL

MEDIUM 90° TAIL

FIXED-FIN TAIL

2.37" ROCKET PROJECTILES
SHOWING C.G. & C.P. LOCATIONS
DRAWN TO SCALE

CONFIDENTIAL

HYDRAULIC MACHINERY LABORATORY CALIFORNIA INSTITUTE OF TECHNOLOGY		
DR	FIG. 16	SCALE
CH		ND 11-585 L
AP		

PRINT NO. 16 ISSUED TO

CONFIDENTIAL